Sports Eng (2013) 16:137–154
DOI 10.1007/s12283-013-0117-z

INVITED PAPER

A review of recent research into aerodynamics of sport projectiles

John Eric Goff

Published online: 28 April 2013

Abstract A review of aerodynamics research connected to sport projectiles is presented here. The review's focus is on work conducted in the current millennium, though deference is made to some classic work still invaluable to modern research. Besides serving as a resource for seasoned scientists and engineers, this article is especially geared toward young investigators who are just beginning careers in sport science. Basic and sophisticated methods are discussed, including vacuum physics, air drag, lift, numerical approaches, trajectory analysis, wind tunnels, and computational fluid dynamics. Eighteen sports are discussed with an eye to future research.

Keywords Aerodynamics · Archery · Arrow · Badminton · Baseball · Basketball · CFD · Computational fluid dynamics · Cricket · Discus · Drag · Football · Golf · Hammer throw · Ice hockey · Javelin · Lift · Rugby · Sepaktakraw · Shuttlecock · Ski jumping · Sport · Soccer · Tennis · Trajectory analysis · Volleyball · Whiffle ball · Wind tunnel

1 Introduction

Over the past generation, the study of sport has established firm footing among other scientific endeavors. Mechanical and computer engineers have been plying their skills to better our understanding of the flight of association footballs (soccer balls to those in the US). Even physicists may include sport among possible career paths, complementing an array of traditional pursuits such as the study of nuclei and fundamental particles. Examples abound in other scientific fields as well.

There are several reasons why sport's scientific profile has risen. The hypercompetitive world of sport drives athletes and coaches to seek the best available training methods. Clubs, associations, and even governments pour money into scientific studies that not only improve training, but equipment as well. Science can make the difference in Olympic events where winning and losing may come down to millimeters or thousandths of a second.

Beyond financial impact and national pride is the fact that many people love to play and watch sport. Future scientists now see sport as one possible career option and current scientists may use sport science as one way to excite young people about science in general. Sport media have increasingly more tidbits of sport science in stories intended for general audiences.

The purpose of this review article is to acquaint tyros to scientific work that has advanced our understanding of the aerodynamics of sport projectiles. Emphasis will be placed on research carried out and published since the commencement of the twenty-first century, though young investigators should be well familiar with classic work, such as Daish's book on sport [1] and Mehta's wonderful review article [2]. Frohlich's recent review [3] of sports physics literature is also invaluable. White's recent book [4] on sport projectiles is also a fine starting point. Those wishing to contribute to our understanding of sport projectile aerodynamics should be familiar with significant recent papers, the leading researchers, and places where they may pursue their research.

This article is organized as follows. Section 2 introduces the basic ways of moving past a vacuum description of sport trajectories. A long home run from 2012 serves as the

J. E. Goff (✉)
Department of Physics, Lynchburg College, 1501 Lakeside Drive, Lynchburg, VA 24501-3113, USA
e-mail: goff@lynchburg.edu

paradigm for the ideas introduced in that section. More sophisticated ways of investigating aerodynamics in sport are then discussed in Sect. 3. A review of research conducted in 18 sports in Sect. 4 comprises the bulk of this review article. A glimpse at the future of aerodynamic work finishes the paper in Sect. 5. To appeal to as wide an audience as possible, both SI and Imperial units will be used throughout this article.

2 The basics

A typical result from vacuum kinematics is the horizontal range of a projectile launched with speed v_0 and angle θ_0 measured from the horizontal. If, for simplicity, the landing height is the same as the launch height, the horizontal range, R, is given by [5]

$$R = \frac{v_0^2 \sin(2\theta_0)}{g}, \tag{1}$$

where the magnitude of the constant acceleration due to gravity is $g = 9.8$ m/s^2 $= 35$ kph/s $= 22$ mph/s (two-digit accuracy).

The range given by Eq. 1 is only approximate, however, when we consider the following example. Giancarlo Stanton hit the longest home run in Major League Baseball (MLB) during the 2012 season. Hitting for the Miami Marlins against the Colorado Rockies on 17 August in Coors Field in Denver, Colorado, Stanton's home run went an estimated 494 ft (151 m), according to an online database of all MLB home runs [6]. The same database has Stanton's home run leaving his bat at $v_0 =$ 116.3 mph (187.2 kph or 51.99 m/s) with launch angle $\theta_0 = 24.9°$. Ignore the meter or so difference between launch and land heights and Eq. 1 gives $R = 671$ ft $= 211$ m. The fact that the vacuum kinematics result gives a horizontal range that is 40 % longer than the actual range makes it abundantly clear that ignoring air resistance is an assumption that cannot be made if one wishes to understand and model the motion of a sport projectile like a baseball.

As a first effort to refine our predicted home-run range, we include a term to account for air resistance. The magnitude of drag force is given by [7]

$$F_D = \tfrac{1}{2} C_D \rho A v^2, \tag{2}$$

where C_D is the dimensionless drag coefficient, ρ is air density (1.225 kg/m^3 at 15 °C at sea level), A is the projectile's cross-sectional area (6.63 in^2 $= 42.7$ cm^2 for a baseball), and v is the projectile's speed. The direction of the drag force is opposite to the projectile's velocity. A simple way to think of Eq. 2 is to recall that $\frac{1}{2}\rho v^2$ is the dynamic pressure in Bernoulli's equation. That pressure multiplied by the cross-sectional area gives a force. Readers are cautioned not to take this simple way of thinking too far because Bernoulli's equation is quite restrictive, valid only for inviscid flows of incompressible fluids. In a sense then, C_D is a factor [8] that includes various effects not seen in Eq. 2. Because of the complex way in which air exerts a force on a projectile, C_D may depend on the projectile's speed, spin rate, and surface characteristics.

For those seeing Eq. 2 for the first time, C_D is often taken as a constant. Even with that simplification, obtaining the projectile's trajectory requires a numerical approach. Fortunately, in these modern times students and researchers alike have easy access to high-speed computation. Even those who do not wish to program their own numerical algorithms may obtain very accurate solutions using powerful software packages like, for example, *Mathematica* and *Maple*.

As we will see, the inclusion of drag is not enough to accurately model the flight of a home run, for we have not accounted for spin. In fact, a baseball hit for a home run leaves the bat with nearly 2,000 rpm of backspin yet lands with only about 25 % of its initial spin [9]. While spinning, the ball causes the air to be asymmetrically whipped down off the backside of the ball. According to Newton's 3rd Law, there is an upward force component called the Magnus force or lift force. The traditional lift force is modeled by [10]

$$F_L = \tfrac{1}{2} C_L \rho A v^2, \tag{3}$$

where C_L is the dimensionless lift coefficient. Like C_D, the lift coefficient is a factor that contains the complicated features of the lift force, meaning it may also depend on the projectile's speed, spin rate, and surface characteristics. Whereas the form of Eq. 3 is quite useful for the study of fixed objects such as airplane wings, the effect of the projectile's rotation, which is what gives rise to the Magnus effect (knuckleball, or low-spin ball, effects will be discussed in Sects. 4.3 and 4.15), is hidden in C_L. Some researches [9, 11] prefer to have the projectile's spin rate, ω, appear explicitly in F_L, especially when the projectile is spherical. This is done by defining a new dimensionless lift coefficient as

$$C_L' = \frac{C_L}{SP}, \tag{4}$$

where the dimensionless spin parameter is given by

$$SP = \frac{r\omega}{v}, \tag{5}$$

which is the ratio of the ball's tangential equatorial speed to its center-of-mass speed. Here, r is the ball's radius. The alternate lift equation then becomes

$$F_L = \frac{1}{2} C_L' \rho r \omega A v. \quad (6)$$

Equation 6 has a slight advantage over Eq. 3 due to spin rate being explicitly given in Eq. 6, but either equation is fine to use.

The free-body diagram for a spherical projectile moving through air is shown in Fig. 1.

The direction of the lift force is usually in the direction of $\omega \times \mathbf{v}$, though it may point opposite that in the case of the reverse Magnus effect (more on that in Sects. 4.5 and 4.15). The magnitude of the buoyant force, F_B, is usually small, but easy to include in a numerical determination of a ball's trajectory. For a baseball, F_B is only 1.5 % of the ball's weight, which is $mg = 5.125$ oz $= 1.425$ N. Keep in mind that the force the air exerts on a projectile is, however complicated, a force that points in a single direction. Splitting that force into the components seen in Fig. 1 is a matter of convention, albeit a popular convention.

Putting the x direction along the horizontal and the y direction along the vertical, the baseball's trajectory lies in the x-y plane. If the ball had spin that was not pure backspin or topspin it would move out of that plane (we ignore asymmetric wake deflection due to asymmetric surface orientations, which average out due to the high spin rate). Newton's 2nd law gives [12]

$$\ddot{x} = -\beta v (C_D \dot{x} + C_L \dot{y}) \quad (7)$$

and

$$\ddot{y} = \beta v (-C_D \dot{y} + C_L \dot{x}) + \left(\frac{4\pi r^3 \rho}{3m} - 1 \right) g, \quad (8)$$

where $\beta = \rho A / 2m$, $v = \sqrt{\dot{x}^2 + \dot{y}^2}$, and a dot signifies one total time derivative. For a baseball, $\beta = 0.00467$ ft^{-1} $= 0.0153$ m^{-1}.

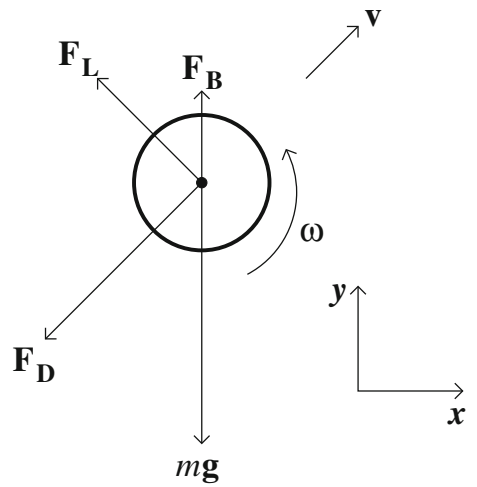

Fig. 1 Free-body diagram showing forces (not necessarily to scale) acting on a spherical projectile with backspin. Note that the direction of ω is out of the page

As noted, the aerodynamic coefficients C_D and C_L are, in general, complicated functions of ball speed, spin rate, and properties of the ball's surface. As a first step beyond the vacuum solution, take C_D and C_L to be constants and solve Eqs. 7 and 8 numerically. For the baseball problem under consideration, $C_D = 0.4$ and $C_L = 0.3$ are reasonable estimates [13, 14].

The vacuum range was 40 % too long. If drag is included, but not lift, the range is 389 ft = 118 m, which is about 21 % short, an improvement, but still indicating the need to include effects from spin. Including both drag and lift, the range is 491 ft = 150 m, which is about 0.5 % short. Figure 2 shows three home run trajectories: vacuum result, drag-only result, and drag and lift result.

Be aware that we are examining a first step away from vacuum kinematics and that the story is far from complete, despite the fantastic 0.5 % discrepancy between our model range and the actual range. Though our estimates for C_D and C_L were obtained from research into baseball aerodynamics, we err by keeping them constant. We have also not accounted for any wind that was present during the home run, air temperature (range goes up with increasing temperature), and relative humidity (range goes up with increasing humidity, though not to the degree that it does with increasing temperature), all of which influence the trajectory. The online database [6] claims that Stanton's home run reached a maximum height of 109 ft = 33.2 m. The maximum height of the drag and lift trajectory shown in Fig. 2 is 108 ft = 33.0 m, which is about 0.6 % too short.

The skeptical reader will note that we have the actual home-run trajectory and that C_D and C_L are two free parameters that we could vary until our numerically determined trajectory was as close to reality as possible. In fact, such a numerical optimization returns values for C_D and C_L that are quite close to what was used above. We may think of such an optimization as determining average values of C_D and C_L. The problem is that such values are perhaps useful for long home runs only, and we have not learned much about how air interacts with a baseball. Still, we have made significant progress from simple vacuum kinematics and the numerical calculations needed to produce Fig. 2 are within the grasp of any university science or engineering student. Those interested in more mathematical details behind basic projectile physics, including perturbative techniques, please consult the fine book by de Mestre [15].

3 Beyond the basics

Despite the appearance of parameters like radius, cross-sectional area, and angular speed, the physics contained in Sect. 2 amounts to solving an equation of motion for a

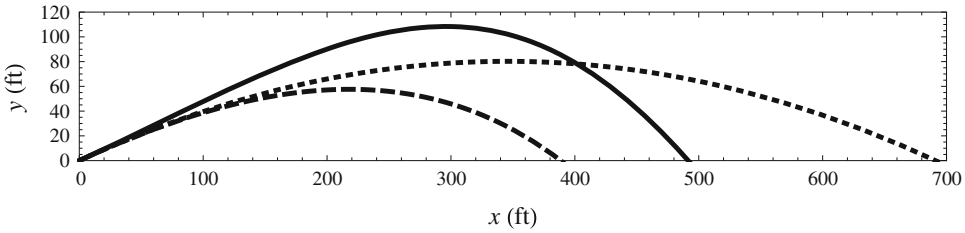

Fig. 2 Model trajectories for Giancarlo Stanton's 494-ft home run. Shown are the vacuum trajectory (*dotted*), drag-only trajectory (*dashed*), and drag and lift trajectory (*solid*)

point particle. To understand the effect a fluid like air has on a projectile during its flight, one must take up the study of fluid mechanics.

Scientific inquiry into aerodynamics took off with Ludwig Prandtl's work at the turn of the twentieth century. A wonderful paper by Anderson [16] describes Prandtl's work, and includes references to seminal articles.

Prandtl introduced the idea of a boundary layer between an object and the free-flowing fluid about the object. Friction, or viscosity, is responsible for fluid adhesion at the object's surface. Moving away from the surface, the velocity gradient is such that at the edge of the thin boundary layer, the fluid velocity is that of the inviscid free-flow fluid (as seen in the object's reference frame). Where the boundary layer separates from the object is a mixing of the shed layer and the inviscid free-flow region. Determining how each element of fluid interacts with the object allows one to calculate the overall force on the object by the fluid. The force on each element of the object has, in general, components parallel to and perpendicular to the object's surface.

To properly analyze an object that moves through a fluid, one must determine the fluid velocity field $\mathbf{v}(\mathbf{r}, t)$, where $\mathbf{r}$ is the position vector for a given fluid element at a particular time t. Using Newton's 2nd law to describe the fluid element and considering the fluid element's volume to make up part of a fluid continuum, one arrives at the famed Navier–Stokes equation [10]. Solutions to this equation yield $\mathbf{v}(\mathbf{r}, t)$ and are aided by making use of a dimensionless parameter, the Reynolds number, Re, given by

$$\mathrm{Re} = \frac{vD}{\nu}, \tag{9}$$

where v is fluid speed far from the object (or object's speed as viewed in a lab frame), D is a characteristic length (diameter for a ball), and ν is the kinematic viscosity, which is $\nu = \mu/\rho$, where μ is the viscosity. The Reynolds number is a qualitative comparison of a fluid's inertia to its viscosity. The beauty of having a dimensionless Navier–Stokes equation with one parameter is that solving the equation for a particular Re gives one an understanding of various-sized objects. Suppose one can guarantee exactly the geometric scale of two objects, say one of size D and the other of size $10D$. Solving the dimensionless Navier–Stokes equation for the former object with fluid speed v yields immediate knowledge about the latter object at speed $v/10$ because both cases lead to the same Re. This is why small-scale models of cars, bridges, airplanes, dams, etc may be used in wind tunnels to give engineers an idea of what will happen to the larger versions of those objects in appropriately scaled velocity fields. A challenge for sport researchers with small wind tunnels is getting fast enough air flows over small-scaled sport objects so as to give useful results for those objects moving at normal game speeds.

At a temperature of 15 °C = 59 °F, air has a sea-level density of $\rho = 1.225$ kg/m^3. Using that density with the viscosity of air, which is $\mu = 1.81 \times 10^{-5}\mathrm{kg}/(\mathrm{m\,s})$ at 15 °C, air's kinematic viscosity is $\nu = 1.48 \times 10^{-5}$ m^2/s. Both ρ and μ decrease as the temperature increases; those interested in finding ν at a temperature other than 15 °C should consult tables [10] of ρ and μ for various temperatures. The Reynolds number for an object moving through air at sea level and at 15 °C is thus

$$\mathrm{Re} \times 10^{-5} = \left(0.677 \frac{\mathrm{s}}{\mathrm{m}^2}\right) vD, \tag{10}$$

indicating that Re $\sim$ 10^4–10^5 for most sport projectiles.

For sport balls, D is simply the ball's diameter. Table 1 lists the sport balls reviewed in this article, along with quick conversions to obtain Re for any speed. Take baseball as an example. From simple tosses around the infield to soon-to-be long home runs coming off the bat, baseball speeds range from about 5 m/s = 18 kph = 11 mph to approximately 55 m/s = 198 kph = 123 mph. Using Table 1, one obtains $0.25 \times 10^5 < \mathrm{Re} < 2.75 \times 10^5$ as a rough estimate of the range of Reynolds numbers for the sport of baseball.

Analytic solutions to the Navier–Stokes equation for real sport objects do not exist. In the middle of the nineteenth century, Stokes derived an analytic solution for the drag force on a nonspinning smooth sphere, but the result is valid only for Re $\ll 1$ (though it often works well for Re $\simeq$ 1). As simple a final result that Stokes found, the derivation is not trivial. Essentially, anything more complicated requires experimental and numerical work.

Researchers find aerodynamic coefficients experimentally using wind tunnels and trajectory analysis. Figure 3

Table 1 Get Re from ball speed for various sport balls. The Re numbers correspond to sea level elevation and 15 °C = 59 °F temperature

Ball	D	Re × 10^{-5}
Baseball	7.38 cm = 2.90 in	v/20.0 m/s = v/72.1 kph = v/44.8 mph
Basketball	24.0 cm = 9.45 in	v/6.16 m/s = v/22.2 kph = v/13.8 mph
Cricket	7.20 cm = 2.83 in	v/20.5 m/s = v/73.9 kph = v/45.9 mph
Golf	4.27 cm = 1.68 in	v/34.6 m/s = v/125 kph = v/77.5 mph
Sepaktakraw	13.7 cm = 5.39 in	v/10.8 m/s = v/38.9 kph = v/24.1 mph
Soccer	22.0 cm = 8.65 in	v/6.73 m/s = v/24.2 kph = v/15.0 mph
Tennis	6.70 cm = 2.64 in	v/22.1 m/s = v/79.4 kph = v/49.3 mph
Volleyball	21.0 cm = 8.27 in	v/7.03 m/s = v/25.3 kph = v/15.7 mph
Whiffle ball	7.00 cm = 2.76 in	v/21.1 m/s = v/76.0 kph = v/47.2 mph

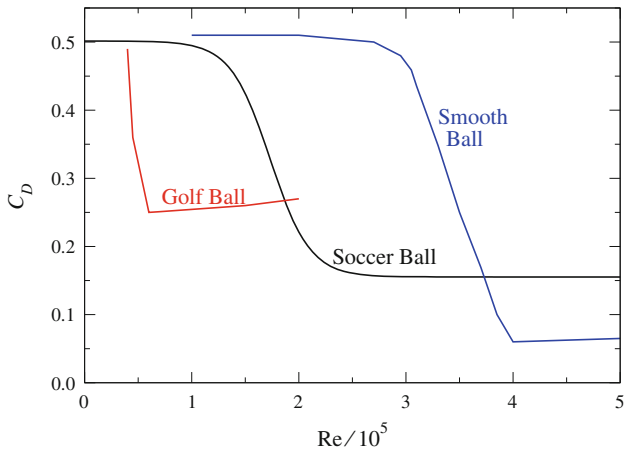

Fig. 3 C_D as a function of Re for a smooth sphere [17], a soccer ball (smoothed data) [18], and a golf ball [19]

shows C_D as a function of Re for a smooth sphere [17], soccer ball [18], and a golf ball [19], all of which have no spin.

The precipitous drop in C_D with increasing Re (or speed) is called the "drag crisis". During that transition region, flow around an object changes from laminar to turbulent. Figure 4 shows a soccer ball with laminar flow; Fig. 5 shows the same ball with turbulent flow. In each figure, the nonspinning ball is moving through a dust cloud so as to show boundary-layer separation.

Note that the boundary layer separates farther back on the ball for turbulent flow compared to laminar flow. Note, too, that the rougher the surface, the smaller Re is where

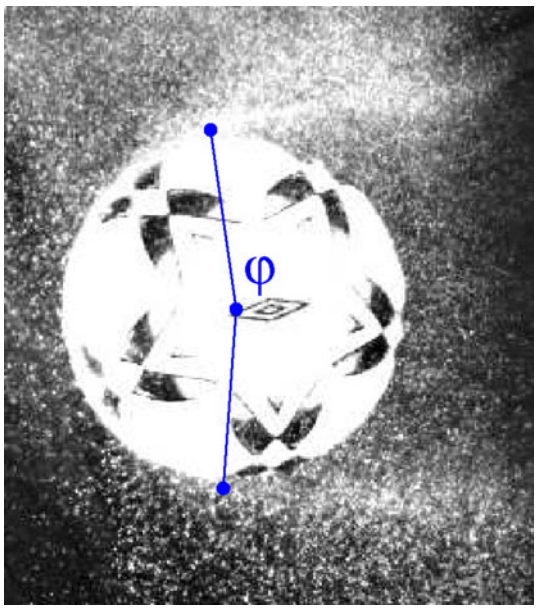

Fig. 4 A 32-panel soccer ball with laminar flow [18]. The ball's speed is 7.65 m/s = 27.5 kph = 17.1 mph, corresponding to Re = 1.14 × 10^5. The ball moves from right to left. The boundary-layer separation angle is $\varphi \simeq 198°$

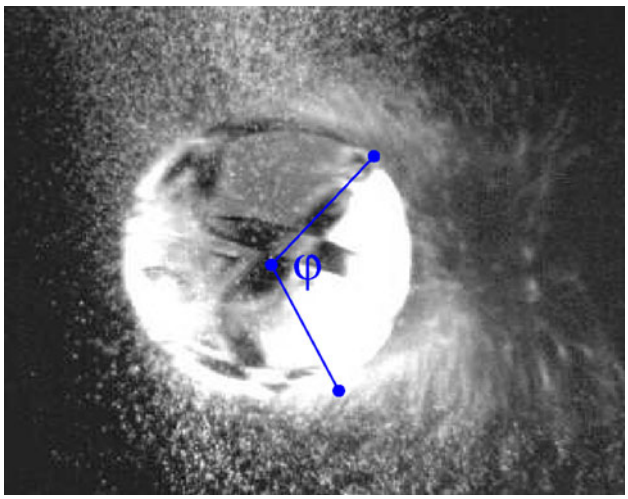

Fig. 5 A 32-panel soccer ball with turbulent flow [18]. The ball's speed is 19.14 m/s = 68.9 kph = 42.8 mph, corresponding to Re = 2.85 × 10^5. The ball moves from right to left. The boundary-layer separation angle is $\varphi \simeq 97°$

the drag crisis occurs. This is why an intentionally roughened surface helps a golf ball travel much farther than it would if it did not have its dimples. Classic [20] and recent [21] research has been done to understand how surface roughness changes aerodynamic coefficients.

For balls with or without spin, having asymmetric geometric area presentations to the oncoming air, the boundary layer will separate asymmetrically behind the ball, leading to a lateral (Magnus) force component.

Newton's 3rd law easily explains this lateral force, linking the direction the ball has deflected with the wake of air behind it. An analogy is that of a boat's rudder asymmetrically deflecting water behind the boat to turn the boat. Spinning balls require the spin parameter, Sp, given by Eq. 5, to aid in the aerodynamic explanation.

To account for the preceding effects, one must employ sophisticated computational techniques. One approach is to replace derivatives in the equations of motion with their finite-difference counterparts [22]. Standard techniques like relaxation methods are then available.

The finite-element method [23] is another computational approach, in which a mesh of geometric shapes is created with node locations where variables of interest are evaluated. This method generates algebraic equations that are usually solved with matrix methods. A method that puts all its elements on the boundary instead of the interior is the boundary-element method [24]. This latter method is quite new and has not made significant strides into sport research.

Because of the availability of many commercial codes, the use of computational fluid dynamics, or CFD, has become a major research tool for those interested in aerodynamics in sport. Investigators can not only determine aerodynamic coefficients like C_D and C_L, but they can also visualize flows and study energy transfers. If research budgets are small, and building a sophisticated wind tunnel is not possible, CFD may be an option for those looking to contribute to sport research.

The process of CFD begins by obtaining a representation of the object in question. Laser scanning is one way to input a geometry into a mesh. Once the mesh is formed, a commercial CFD code may be used to solve the Navier–Stokes equations, as well as other equations of interest. Post-solution processing is then needed to take the numerical solution and create flow-field images and animations.

A nice, short review of CFD in sport is given by Hannah [25]. For those interested in all the details of CFD, Chung's tome [26] has more than enough to keep an investigator busy for quite some time.

4 Recent research progress

What follows is a survey of recent investigations into aerodynamics of sport projectiles. The summary for each sport is not meant to be anything close to a comprehensive review, but rather a précis of recent significant results. Space limits discussion to a few articles for each sport. The hope is that researchers will be able to glimpse recent research successes in a given sport, and then access references for more details.

4.1 Archery

The popularity of the book and movie *The Hunger Games* may have helped boost television ratings for archery at the 2012 Summer Olympics in London [27]. Research into the aerodynamics of shot arrows has increased considerably in the past decade, adding many references to classic work [28]. Novice researchers may find a suitable starting point to be a popular science book [29].

Due to its elongated shape and sometime wobbly flight, determining an arrow's speed is a nontrivial experimental challenge. One US group [30] used the Doppler effect to determine speed. They fitted arrows with tips designed to make high-frequency whistles, and then shot the arrows over microphones.

Recent progress has also been made by researchers in Australia. After an exhaustive study of the arrow leaving the bow [31], the group turned to aerodynamic properties of the arrow in flight. One experiment [32] involved a scale-model arrow in a water channel in which the transition from laminar flow to turbulent flow was seen for $\mathrm{Re} \simeq 4.5 \times 10^4$.

A more extensive investigation [33] examined drag contributions from four parts of the arrow: fletch, shaft, nock, and point (see Fig. 6). Arrows were shot through a chronograph to determine speeds at particular distances. Those speeds compared well with model predictions. The comparison between predicted arrow rotations and actual rotations fared well, too.

A group in Japan [34] used both a wind tunnel and trajectory analysis to extract aerodynamic properties of arrows in flight. Arrows were fitted with both bullet and streamlined tips. To avoid the problem of attaching the arrow to a support rod, the group inserted magnetic materials into the arrow's shaft and then magnetically levitated the arrow while in the wind tunnel. Optical sensors and the ability to control the strength of the magnetic field so as to maintain the arrow in a fixed position allowed the researchers to measure aerodynamic forces and then extract from those force measurements the aerodynamic coefficients in Eqs. 2 and 3. Also of interest to those who investigate arrows is the pitching moment, τ_M, which arises when the aerodynamic force is at the aerodynamic center instead of the center of pressure, and is given by

$$\tau_M = \frac{1}{2} C_M \rho A v^2 L, \tag{11}$$

Fig. 6 A quick way to get Re for an arrow is to set D in Eq. 9 equal to the mean shaft diameter. One research group [33] gets drag contributions from the four *labeled* parts of the *arrow*

where L is the arrow's length and C_M is the dimensionless pitching moment coefficient. Their wind-tunnel experiments were conducted for $0.4 \times 10^4 < \mathrm{Re} < 1.5 \times 10^4$, corresponding to a top speed of about 45 m/s = 162 kph = 101 mph, which is roughly 75 % the speed of a typical arrow. Air flow remained laminar in their tested wind-tunnel range with $C_D \simeq 1.5$ for $1.0 \times 10^4 < \mathrm{Re} < 1.5 \times 10^4$. Increasing wind-tunnel air speed to allow investigation of the transition from laminar to turbulent flow is of interest.

The Japanese group's trajectory analysis experiment used two cameras 45 m apart and lift-free arrow flights. Instead of filming an arrow's entire trajectory, they linked data from each of the two cameras to extract the aerodynamic coefficients. Their trajectory analysis experiments were performed for $0.9 \times 10^4 < \mathrm{Re} < 2.4 \times 10^4$. These experiments showed a transition from laminar to turbulent flow for $\mathrm{Re} \simeq 1.3 \times 10^4$, smaller than the Australian group's water-channel experiment, with a corresponding increase in the drag coefficient to about 2.6 at $\mathrm{Re} \simeq 2.4 \times 10^4$. Reducing error in the trajectory analysis is needed, as well as a better description of what happens at the transition from laminar to turbulent flow to make the drag coefficient increase by 33–67 %.

Engineers in the US and Ireland [35] are now fitting arrow tips with a tiny sensory data acquisition system that allows for real-time ballistic information. It will be of great interest to see how these devices develop and if they are implemented into archers' training.

Promising finite-difference and finite-element work [36] has already investigated arrow vibration. It seems that much CFD work with arrow aerodynamics remains to be performed. The task will probably involve laser scanning of an arrow if one wishes to move beyond a simple cylinder geometry.

4.2 Badminton

Like the arrow used in archery, badminton's shuttlecock has a complicated geometry. A Taiwanese group [37] used a video camera and equations of motion to determine a shuttlecock's terminal speed, which they found to be 6.86 m/s = 24.7 kph = 15.3 mph. Given that smashes in badminton give the shuttlecock initial speeds up to about 75 m/s = 270 kph = 168 mph, air drag is an incredibly important force to understand if one wishes to accurately describe shuttlecock trajectory.

An Australian research group [38] conducted wind-tunnel measurements on various shuttlecocks, some feather and some synthetic. Air speeds varied from 16.7 m/s = 60 kph = 37.3 mph to 33.3 m/s = 120 kph = 74.6 mph, corresponding roughly to $0.7 \times 10^5 < \mathrm{Re} < 1.5 \times 10^5$ (see Fig. 7). Averaging over shuttlecock type, the group found C_D to increase from about 0.5 at the smallest Re to about 0.65 for $\mathrm{Re} \simeq 10^5$. From there, C_D drops to about 0.6 at $\mathrm{Re} \simeq 1.2 \times 10^5$ and levels off. Readers are encouraged to examine the group's paper [38] for variations in C_D with shuttlecock type.

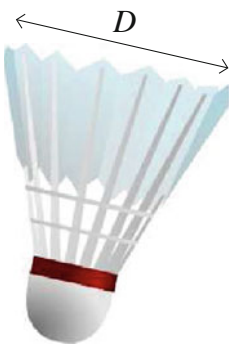

Fig. 7 A standard way to get Re for a shuttlecock is to set D in Eq. 9 equal to the skirt diameter

A US study [39] found drag coefficients similar to the Australian work. The former group used roughly the same lower limit on Re in their wind tunnel, but went to $\mathrm{Re} \simeq 2.1 \times 10^5$ at the upper end, noticing a very gradual decrease in C_D as Re increased past $\mathrm{Re} \simeq 10^5$. For large Re, the US group speculated that skin (i.e., surface) friction dominates the air drag. Their experiments also accounted for players' desire to use feather shuttlecocks over synthetic plastic. At large speeds, plastic shuttlecock skirts experience considerable deformation, leading to smaller drag and faster shuttlecocks.

The US group furthered its investigation by spinning the shuttlecock in the wind tunnel. They noticed a Magnus effect and found C_L to rise from 0.15 at $\mathrm{Sp} \simeq 0.1$ to about 0.20 at $\mathrm{Sp} \simeq 0.2$, which is a range of Sp typical of normal play. Shuttlecock drift noticed by players is explained by the presence of a Magnus effect.

Further studies in a Japanese wind tunnel [40] confirmed aforementioned C_D values and showed that if the gaps in the feathers were closed, C_D drops to about two-thirds of its normal value. The group also used smoke to visualize flow patterns around the shuttlecock at $\mathrm{Re} \simeq 2.1 \times 10^5$, corresponding to a speed of 50 m/s = 180 kph = 112 mph. Flow patterns were similar for nonspinning and spinning shuttlecocks, confirming wind-tunnel results that C_D is not a strong function of spin.

A French group [41] studied the flip of the shuttlecock using high-speed video. The flip takes places after the racket hits the shuttlecock and occurs about 20 ms after the hit.

What is needed in the aerodynamic study of shuttlecocks is CFD work, which is made challenging by the shuttlecock's geometry.

4.3 Baseball

Researchers have been studying the aerodynamics of baseballs for more than half a century, dating back to classic wind-tunnel work done by Briggs [42]. The 6-ft (1.83-m) wind-tunnel Briggs employed examined speeds as large as 150 ft/s (45.7 m/s = 165 kph = 102 mph), such that the maximum Reynolds number was $\mathrm{Re} \simeq 2.3 \times 10^5$, and spins that reached 1,800 rpm, corresponding to $\mathrm{Sp} \simeq 0.15$ at maximum speed. Instead of recounting the main contributions of efforts in the twentieth century to understanding baseball aerodynamics, tyros should consult a couple of now classic books [9, 13] on baseball physics to get a feeling for the sizes of the drag and lift coefficients.

Research groups in this century have improved our understanding of baseball aerodynamics with the use of high-speed cameras in experiments and by accessing vast reservoirs of online data of real baseballs in flight. A California (US) research group [43] used seven cameras to record the initial flight of a pitch and three cameras near home plate. Using trajectory analysis on two- and four-seam fastballs, the group determined C_L for spin parameters roughly in the range $0.1 < \mathrm{Sp} < 0.5$.

The California group then published work [44] on ways to optimize bat swing to maximize the range of batted baseballs. They found that balls hit long distances go through the drag crisis at $\mathrm{Re} \simeq 1.6 \times 10^5$, which corresponds to a ball speed of 32 m/s = 115 kph = 72 mph. The group also found that curveballs could be hit farther than fastballs because the topspin imparted on the baseballs by pitchers results in more topspin on the batted ball, thus increasing lift.

Nathan [14] used high-speed cameras and trajectory analysis to investigate C_L up to $\mathrm{Sp} \simeq 0.6$. For baseball speeds below the drag crisis, $C_\mathrm{L} \simeq \mathrm{Sp}$. For speeds comparable to game play, which are in the drag crisis and beyond, $0.15 < \mathrm{Sp} < 0.25$, $C_\mathrm{L} \simeq 0.2$ and does not depend strongly on ball speed if Sp is constant. Further work [45] has examined how the lift force on the ball makes it challenging to catch pop ups.

Nathan has made extensive use of PITCHf/x trajectory data for every Major League pitch, which may be accessed online [46]. One example is his recent investigation [47] into the aerodynamics of knuckleballs, i.e., balls with little to no spin. By examining trajectory data for a few Major League knuckleball pitchers, Nathan found knuckleball pitch movement to be random, but as smooth as any other type of pitch. New researchers interested in analyzing baseball trajectories are urged to investigate online PITCHf/x data.

A Colorado (US) group [48] studied the effect of storing baseballs in humidors, which has been done in Denver, Colorado for more than a decade to compensate for the low air density at mile-high elevation. The group measured how baseballs change in size and weight after being stored in humidors, and then modeled trajectories with new size and weight parameters. They found that wetter curveballs break slightly more, about 0.5 cm = 0.2 in, and travel slightly farther, by about 0.6 m = 2 ft. They also noted that wetter balls may allow pitchers to spin them better, thus increasing lift on fastballs and curveballs.

Level of ball wetness and pitcher-imparted spin influence batted trajectories, but the main influence is obviously the ball–bat interaction. Recent work [49] has been done to categorize how the ball leaves the bat for various impact angles.

We are marching closer to the true path of a baseball. As with archery arrows, baseballs are now being fitted with miniature electronic devices to obtain trajectory information [50].

4.4 Basketball

Those wishing to begin researching basketball physics might start with a general-audience book [51], in which basic aerodynamics is discussed. The game of basketball involves a great deal of dribbling and short-distance passing; gravity dominates much of that play. With the exception of the occasional half-court shot as time expires, most long basketball shots have launch speeds not more than about 15 m/s = 54 kph = 34 mph, which corresponds to $\mathrm{Re} \simeq 2.5 \times 10^5$. With backspin on most shots, a three-point shot might have $\mathrm{Sp} \simeq 0.12$ or thereabouts. Drag forces on long shots could initially be as large as half the ball's weight; lift forces could near 10 % the ball's weight. Such long shots represent the extreme for normal basketball trajectories. All two-point shots have smaller launch speeds and consequently smaller drag and lift forces. Players use repetition and muscle memory to develop visceral knowledge of optimum launch speeds and angles for various shot locations on the court.

Researchers [52] have developed models for optimum shooting parameters for various shot types, ignoring drag for shots near the basket. The spin of the ball plays a significant role when examining shot success when the ball bounces off the backboard. Dynamic models have also been created [53] that determine the best rebounding positions based on a randomized set of initial shot parameters.

4.5 Cricket

In addition to the cricket discussions in his review article [2], a delightful and informative article on cricket aerodynamics was authored in the past decade by Mehta [54]. In that article, he describes the swing (i.e., lateral

deflection) of a cricket ball after being released by the bowler. The idea is to have the ball move at such a speed that if not for the seams, the boundary layer would be entirely laminar. The bowler spins the ball such that the seams form the "equator" of the spinning ball and the spin axis neither points in the direction of the ball's velocity nor perpendicular to that axis. The asymmetric presentation of the seams to the oncoming air is the key to swing. The boundary layer remains laminar on the smooth part of the ball; the seams induce the laminar layer into turbulence. Because the turbulent boundary layer separates farther back on the ball compared to the laminar boundary layer, there is a force toward the turbulent side of the ball. That sideways force gives rise to swing. Mehta [54] illustrated the asymmetric separation with smoke over the ball in a wind tunnel.

Perhaps more interesting than ordinary swing is reverse swing. Mehta [54] provides a nice qualitative description of the phenomenon. Ball spin and orientation are just as described for ordinary swing, only now the ball must be thrown fast enough that the boundary layer is turbulent over the entire ball. In that situation, the seams enhance the thickness of the boundary layer, which weakens it, causing it to separate sooner than if there were no seams. The asymmetric boundary-layer separation is now opposite to the ordinary case, leading to a force in the direction of the non-seam part of the ball. Figure 8 illustrates how the boundary layer separates from a cricket ball with reverse swing.

Mehta notes that speeds must be upwards of 40 m/s = 144 kph = 89 mph to see reverse swing, meaning only the elite bowlers could do this. Lower-speed bowlers could still achieve reverse swing if they used a worn ball, meaning the surface is rougher than a new one, which pushes the drag crisis to a lower speed. Mehta suggests that speeds around 30 m/s = 108 kph = 67 mph would give reverse swing with a worn ball.

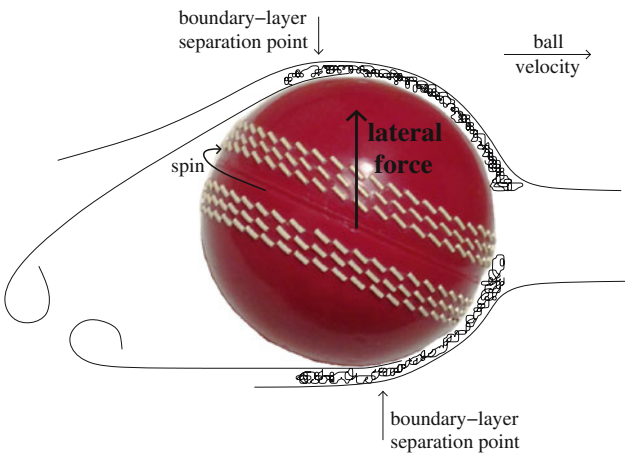

Fig. 8 Reverse swing on a high-speed cricket ball that moves left to right. This figure is adapted from Mehta's work [54]

Beyond normal aerodynamics, playing surface and atmospheric conditions may influence cricket play. One study [55] used high-speed video and more than 3,000 bounces to analyze ball rebounds off several different pitches. Of the various results contained in that study, one qualitatively obvious result that the researches made quantitative is that pitches with large concentrations of clay lead to smaller rebound speeds compared to pitches with small clay concentrations. Another study [56] could not find strong correlation between atmospheric humidity and swing bowling.

As with aforementioned arrows and baseballs, cricket balls can be fitted with interior electronics that allow for the determination of parameters crucial to aerodynamic effects. An Australian group [57] uses internal electronics to ascertain spin rates up to 55.5 rps = 3330 rpm about any of the three axes.

Seminal CFD work [58] on cricket balls used finite-element meshes for two- and three-dimensional geometries. Software restrictions on the use of hexahedrals instead of wedges and computational memory and speed limits gave incomplete pictures of the three-dimensional flow. The researchers were, however, able to see both types of swing in their CFD studies.

4.6 Discus and discs

Recent work [59] on discus trajectories has considered the full three-dimensional problem of a spinning discus, thus extending classic two-dimensional work [60]. The three-dimensional model allows for $C_M \neq 0$ (see Eq. 11), which means angular momentum may precess, thus changing the attitude (i.e., orientation) of the discus. Optimizing the initial conditions with a launch speed of 25 m/s = 90 kph = 56 mph gives optimal ranges of 69.39 m = 227.7 ft for the 2-kg men's discus (see Fig. 9) and 72.13 m = 236.6 ft for the 1-kg women's discus. Those results correspond to 6.33 % short of the men's record held by Jürgen Schult and 6.08 % short of the women's record held by Gabriele Reinsch. Wind might explain some of the discrepancies because headwinds may help improve range, whereas tailwinds may reduce range. For more qualitative explanations, readers may consult a general-audience book [61].

More recently, a Japanese group [62] measured C_D, C_L, and C_M in a wind tunnel for various attack angles. They found little dependence on air speed and on Sp for a given speed. Smoke and oil flows over a discus helped visualize the air's velocity field.

There has also been recent interest in sport discs, such as a Frisbee. Using a three-dimensional model with six degrees of freedom, a UK group [63] found that rotational speed decay may be ignored and that pitching the disc at about 10° maximizes range, whereas pitching it at around

Fig. 9 End view (*top*) of a men's 2-kg discuss presents minimum cross-sectional area, which is about one-sixth of the maximum cross-sectional area (*bottom*) of 0.038 m^2 (0.41 ft^2)

20° will maximize flight time. A US group [64] determined maximum ranges for a launch speed of 30 m/s = 108 kph = 67 mph to be 186 m = 610 ft for a "wings level" (i.e., no bank) disc and 157 m = 515 ft for a free disc (i.e., one free to have any orientation).

As amateur interests in Ultimate Frisbee and Disc Golf increase, research into sport discs is sure to grow as well.

4.7 Football

American football is played with a ball similar in shape to a prolate spheroid. Aerodynamics plays a role in passes and kicks; the rest of the game is played mostly with the ball tucked in a player's arm. For those interested in an introduction to the science of American football, there are general-audience books [65, 66] available.

Modeling the flight of an American football is challenging because of the various orientations the ball may present to the air. Even tight spirals present challenges because the stitches provide an asymmetric mass distribution that causes the direction of the angular momentum vector to change and the trajectory of the ball to drift out of a plane. For kicks and poorly thrown passes, the ball wobbles and tumbles, leading to extremely complicated interactions with the air.

Analytic and numerical work [67] has been done to model the football's trajectory. Equations of motion are sufficiently challenging, but interesting conclusions were reached, such as the fact that stabilization that arises with the ball's spin helps keep the ball's nose roughly oriented along the flight path.

Past wind-tunnel experiments have not yielded consistent drag coefficients. One study [68] has $C_D = 0.16$ for the ball oriented in the position of a tight spiral, i.e., the minimum-area projection; for the maximum-area projection (rotate the ball 90° from minimum-area projection), $C_D = 0.85$. Another study [69] found $C_D = 0.19$ for the minimum-area projection and $C_D = 0.75$ for the maximum-area projection. For normal passes, speeds are large enough that flow over the football is turbulent, so C_D should not be a strong function of ball speed. For a discussion of why C_D decreases with ball spin, see a US wind-tunnel study [70].

More wind-tunnel experiments are needed, as is better flow visualization while the ball is spinning. A quality CFD study of the American football is lacking.

4.8 Golf

A golf ball is the quintessential rough ball with a surface covered in dimples that reduce drag and allow for long drives. A good general-audience book on golf physics is available [71]. There are a couple of classic papers [19, 72] describing wind-tunnel investigations into the aerodynamics of golf balls that are required reading for new investigators. One [19] of those studies clearly established that the drag crisis for a golf ball occurs for $4 \times 10^4 < \mathrm{Re} < 6 \times 10^4$.

A recent Korean experiment [73] sought to understand how dimples reduce drag on balls like those used in golf. Those researchers quantified how dimple depth affected the drag crisis. Using shallower dimples than in one of the classic studies [19], the Korean scientists found that the Reynolds numbers associated with the drag crisis increased as dimple depth decreased. They produced time-averaged velocity profiles near the ball's surface to demonstrate the reduction in C_D as speed increases through the drag crisis. Past the drag crisis where C_D is small, they found bubbles forming inside the dimples. As the bubbles separate from the ball, they help delay the separation of the boundary layer.

Because equipment rules are nowhere near as strict in golf as for a sport like baseball, companies are willing to invest a great deal of money into equipment research and development. As an example of some research that delves into the equipment, a Canadian scientist published two papers [74, 75] at the beginning of this century that dealt with the driver's interaction with the ball. The optimum dynamic loft goes down with increasing impact speed. Such a result is important when designing the curvature of the driver's club head.

A computational discussion of turbulent flow around a golf ball appeared in a more general paper [76] on early uses of supercomputers to aid in solving turbulent-flow problems. More recently, a Japanese group [77] has created a finite-element model of the club shaft while in motion and of the club's impact with the ball. The model uses an approximate geometry for the club and a core/mantle/cover geometry for the ball. The group's computational model agreed quite well with experimental data taken from high-speed video.

4.9 Hammer throw

The hammer is comprised of a metal ball attached to a steel wire that cannot be longer than 1.22 m = 4.00 ft. Women use a 4-kg ball; men use a 7.26-kg ball. The aerodynamics of the hammer in flight are thus more complicated than simply that of a smooth sphere. Though the hammer throw has not been studied nearly to the extent of, for example, soccer balls in flight, a modest amount of research has been performed. A study [78] in the last decade looked at the modeling implications of where one takes the center of mass in the ball/handle/wire system. The study also found that the ball and the handle/wire combination contribute roughly the same amount to the drag force.

An interesting line of research might be to compare the aerodynamic properties of a traditional hammer with the one used for the Scottish hammer throw in the Highland games. The latter hammer often uses a wooden shaft instead of a steel wire.

4.10 Ice hockey

Though most of the game of ice hockey is played with the puck on the ice, there are occasions when the puck is slapped such that it is a projectile through the air. A great general-audience book [79] is available for those interested in learning about basic physics in ice hockey.

For the range $1.3 \times 10^5 < \mathrm{Re} < 3.1 \times 10^5$, corresponding to speeds ranging from 13.3 m/s = 47.9 kph = 29.8 mph to 30.1 m/s = 108 kph = 67.3 mph, a German research group [80] found that C_D, C_L, and C_M are roughly constants with mean values $C_D = 0.76 \pm 0.02$, $C_L = 0.61 \pm 0.02$, and $C_M = 0.039 \pm 0.003$. Wind-tunnel tests were done with a 40° angle of attack. Because there was not much dependence on Re, the group measured C_D, C_L, and C_M for many other attack angles.

The German group then simulated many puck trajectories to see which initial conditions led to pucks leaving the playing area. They also examined impact pressures on the skull so as to ascertain the safety level of different board heights. Simply increasing the height of the protective glass above side walls from 0 to 2.63 m = 0.802 ft drops the frequency of spectators getting hit by 77 %.

The complicated tumbling of the puck through the air suggests that an accurate CFD study will be very challenging.

4.11 Javelin

Much of the classic work on javelin aerodynamics, both before [81, 82] and after [83–85] the rule change in the mid 1980s that moved the center of mass forward 4 cm = 1.6 in so as to reduce range and ensure safer landings, remains standard reference material today. Hubbard played a key role in that classic research. Today's javelin is 2.6–2.7 m (8.5–8.9 ft) long with a mass of 0.8 kg for men; women use a javelin 2.2–2.3 m (7.2–7.5 ft) long with a mass of 0.6 kg. The maximum shaft diameter D, which is used in Eq. 9 to determine Re, is 3.0 cm (1.2 in) for men and 2.5 cm (0.98 in) for women. What the aforementioned classic research taught us is that a pitching moment exists because the center of mass is not at the same location as the center of pressure. A men's javelin is thrown with a speed around 30 m/s = 108 kph = 67 mph, and has an optimal range of about 100 m = 328 ft if thrown at about 30° above the horizontal [83]. That range exceeds the vacuum range because lift enhancements exceed drag reductions. Aerodynamic forces are smaller in the first part of the javelin's motion compared to the latter part as the attack angle grows. Though javelin angular speeds are small, of the order of 10°/s, the range is quite sensitive to fluctuations in the angular speed [81]. Vibrational modes in the javelin increase both the drag and lift forces compared to javelins thrown with no vibrations [84].

Research into javelin aerodynamics has been somewhat sparse in the current century. A group in Poland [86] performed trajectory modeling that gave similar results to the aforementioned classic work. Another Polish group [87] used neural networks to match model range predictions for specific athletes to their actual ranges, thus establishing a means of predicting throwing ability for a particular athlete. It will be nice to see future CFD work on javelins that accounts for vibrational modes as well as aerodynamic forces.

4.12 Rugby

A rugby ball has a similar prolate spheroid shape to that of an American football, but is slightly larger. For those unfamiliar with rugby, a delightful general-audience book [88] awaits you.

A Japanese group [89] performed wind-tunnel tests on a full-size rugby ball. Magnus forces were measured by spinning the ball along its longitudinal axis. They found values of C_D, C_L, and C_M for various attack angles, speeds between 15 m/s = 54 kph = 34 mph and 30 m/s = 108 kph =

67 mph, and spin rates between 60 and 600 rpm. They determined empirical polynomial fits to the aerodynamic data for the various coefficients. Aerodynamic stall occurs for an attack angle around 60° and a ball will deviate from a plane even if the linear and angular velocities are parallel.

Wind-tunnel and CFD work [90, 91] out of Australia has produced aerodynamic coefficients and flow visualizations for rugby balls (Australian rules footballs, too). Speeds in the range 11 m/s = 40 kph = 25 mph to 39 m/s = 140 kph = 87 mph were tested and modeled. As an example of their work, a wind-tunnel test of a nonspinning ball with zero attack angle led to $C_D = 0.18$; the same setup in the CFD analysis gave $C_D = 0.14$. They found that as attack angle increased, the discrepancy between wind-tunnel and CFD predictions increased, reaching a maximum discrepancy around 60° attack angle. Wind-tunnel and CFD results are similar, but, as the authors noted, three-dimensional scans of rugby balls will be needed to make CFD work even more in line with wind-tunnel experiments.

4.13 Sepaktakraw

The game of sepaktakraw is a kind of kick volleyball that is popular in southeast Asia. The ball is spherical in shape, but is made of a woven layer with 12 holes and 20 interconnections, usually made of rattan or a synthetic fiber. The ball may also be covered with synthetic rubber or some other soft material to dampen the maximum impact force on a player's body.

A Malaysian group [92] examined new balls that use plastic infused with rubber; the new design was supposed to reduce head injuries. The group performed a CFD study and found C_D and C_L for speeds ranging from 10 m/s = 36 kph = 22 mph up to 40 m/s = 144 kph = 89 mph. At the bottom of that speed range $C_D \simeq 0.8$; at the top $C_D \simeq 0.6$. Lift coefficients are at least an order of magnitude smaller. The group found that new balls traveled at higher speeds compared to the old balls, thus agreeing with players who noticed that new balls did not reduce head injuries as they were advertised to do.

The complex surface of a sepaktakraw ball is sure to be studied in greater earnest in years to come.

4.14 Ski jumping

Human beings, plus their skis, clothing, and helmet, are the projectiles of interest in ski jumping. Such projectiles are clearly not well modeled by a single, simple geometric shape, like a sphere or cylinder.

One Japanese study [93] created a force database using a full-scale human model in a wind tunnel. Both flight and landing phases were analyzed. Wind-tunnel speeds up to 25 m/s = 90 kph = 56 mph were employed. The group's paper contains a table of polynomial coefficients for various attack angles, athlete-forward-lean angles, and ski-opening angles. They found, on the one hand, that if the angle of attack is small, C_D and C_L were essentially unaltered by the ski-opening angle. If, on the other hand, the attack angle is large, there is significantly more lift with a V-style ski arrangement compared to parallel skis. Maintaining a V-style orientation is beneficial as one nears the ground due to enhanced lift and reduced drag. The Japanese group attributes the aforementioned benefits to the reduced downwash in back of the skier; closeness to the ground being responsible for the downwash and the V-style responsible for downwash reduction.

Another Japanese study [94] optimized the equations of motion to find the best jump. The researchers found that the V-shape of the ski-opening is best achieved during the first half of the flight, whereas the ski-opening angle should remain constant over the second half. Making use of the previous study [93], the group found that controlling the ski-opening angle is more critical than controlling the forward-lean angle. For little wind, a lean angle of about 7° works well. Headwinds require jumpers to control their ski-opening angle over a wider range compared to what is required when jumping with tailwinds.

Quality CFD work on ski jumping was performed by a Norwegian group [95]. A 1.76-m = 5.77-ft model skier was created in a sequence of steps such that joints are singular points of rotation. Skis of length 2.48 m = 8.14 ft and width 11 cm = 4.3 in were then attached to the virtual skier. Making use of left–right symmetry, half the virtual skier contains nearly a quarter million grid points. The researchers were able to vary the lean and ski-opening angles. Velocity-field visualizations revealed swirls near the front of the skis, leading the investigators to suggest a new ski design with an asymmetric tip.

Aerodynamic work [96, 97] on ski jumping has also been done to aid in the safety and design of winter parks used by amateur enthusiasts. Parabolic landing areas that transition into straight slopes appear to lessen impacts. New work should infuse recent wind-tunnel and trajectory work with terrain models so as to help design fun and safe park jumps. Additional research could couple aerodynamic advances with techniques used to improve training, such as the Swiss study [98] that described the placement of sensors on skiers to help with take-off performance.

4.15 Soccer

It should come as no surprise that the world's most popular sport has been subject to an enormous amount of scientific inquiry. With a new ball released for the World Cup every four years comes the usual controversy and complaints from players. Researchers obtain the new ball and put it

through all kinds of tests. Sports journals abound with articles on association football, or soccer, as it is known in the US and as it will be refereed to in this section to distinguish the sport from American football. Some articles even appear in more general physics or engineering journals. It is therefore impossible to give a comprehensive review of soccer aerodynamic research in the space here. Instead, a look at a few aerodynamic studies from the past decade that cover various investigative approaches will be presented. Despite the effort for economy, this subsection is the longest of Sect. 4 due to the copious research into and popularity of soccer.

The World Cup has seen quite an evolution in ball design just within the past three competitions; all balls have been supplied by Adidas. The 2002 World Cup in Japan and Korea used the Fevernova ball, which had the classic rounded truncated icosahedron design with 20 regular hexagonal panels and 12 regular pentagonal panels. The Teamgeist ball used in Germany for the 2006 World Cup departed from the classic 32-panel design with 14 thermally bonded panels. For the 2010 World Cup in South Africa, Adidas released the Jabulani ball, which had just eight thermally bonded panels. The continued reduction in panels meant a reduced presence of seams. The Jabulani ball was thus covered with grooves to roughen the surface enough to approximate aerodynamic properties of previous balls. Researchers at Loughborough University in the UK played a significant role in the development of the past two World Cup balls. When Adidas unveils the Brazuca ball for the 2014 World Cup in Brazil, there will surely follow numerous aerodynamic ball tests by researchers from around the world.

There are general-audience books [11, 99] available for those just beginning soccer research. For more sophisticated treatments, trajectory analysis is a good place to start. One could insert values for C_D and C_L into Eqs. 7 and 8, numerically integrate, and produce trajectories, much like the ones in Fig. 2. Better yet, one could determine C_D and C_L from Eqs. 7 and 8 if one has filmed trajectory data in hand. One study [12] showed how this is done for two- and three-dimensional motion. A challenge of such an approach is obtaining accurate velocity and acceleration components numerically from position coordinates obtained via high-speed video. The aforementioned study discussed one means of smoothing out numerical instabilities, a possible improvement over previous work [100] that smoothed raw data with quadratic-time functions, which meant that acceleration would be rendered constant over the range of analysis. A follow-up study [101] by the former group determined C_L for a Teamgeist ball up to $Sp \simeq 1$, beyond the range of most wind-tunnel experiments, which is one advantage of the trajectory-analysis approach (another being the lack of the need of a bar to support the ball, which influences aerodynamics). The group found that for speeds near and beyond the drag crisis C_L increased until $Sp \simeq 0.3$ and then leveled off to values in the range $0.35 < C_L < 0.40$ as $Sp \to 1$. Recent work [102] used trajectory analysis and real kicks filmed with high-speed cameras to glean information about how the ball's surface geometry influences its trajectory. More recent work [103] employing perturbative approaches suggested the need to use a three-dimensional model in the analysis of trajectories. Given the current level of accuracy of camera-supplied position data, and the subsequent need to smooth the data to extract aerodynamic coefficients, it is not clear that using strictly three-dimensional mathematical models is significantly better than employing a two-dimensional model.

Specific kicks in soccer have been modeled. One UK study [104] modeled a direct free kick and found that for a player 18.3 m = 60 ft from the goal and launching with a speed of 25 m/s = 72 kph = 45 mph, the ball should have sidespin and an elevation angle constrained between 16.5° and 17.5° if the player is to have success scoring. A US study [105] modeled not only a free kick, but a corner kick as well. The group mined four-dimensional parameter space formed by the ball's initial launch speed, launch angle, spin rate, and angle from center with the aim of ascertaining success rate for a particular type of kick, either a free-kick goal or reaching a parallelepiped in front of the goal for a corner kick. They found the following rules of thumb for success: 1 in 10 for a free kick and 1 in 4 for a corner kick.

Several wind-tunnel experiments have been performed on soccer balls of various types. Highlighting just a few here, work out of Japan has been particularly fruitful. One study [106] measured the dependence of C_D on Re and Sp on Fevernova, Roteiro, and Teamgeist balls. The drag crisis occurs at $Re \simeq 2.2 \times 10^5$ for Fevernova and Roteiro balls, but at $Re \simeq 3.1 \times 10^5$ for Teamgeist balls. The group measured C_D past the drag crisis up to $Sp \simeq 0.3$ and found that though C_D essentially doubled over that range of Sp, there was no speed dependence. By covering balls with tetrachloride and filming them while they were kicked at a goal, the group could also visualize aerodynamic flow. They examined boundary-layer separation at various speeds below and above the drag crisis.

Another way to visualize boundary-layer separation is with dust. One group [107, 108] fired soccer balls into dust clouds and recorded the ball's path with high-speed cameras. The group was able to determine separation points on nonspinning 32-panel balls just below, through, and just past the drag crisis. Separation moved back on the ball as speeds increased through the drag crisis, with the exception

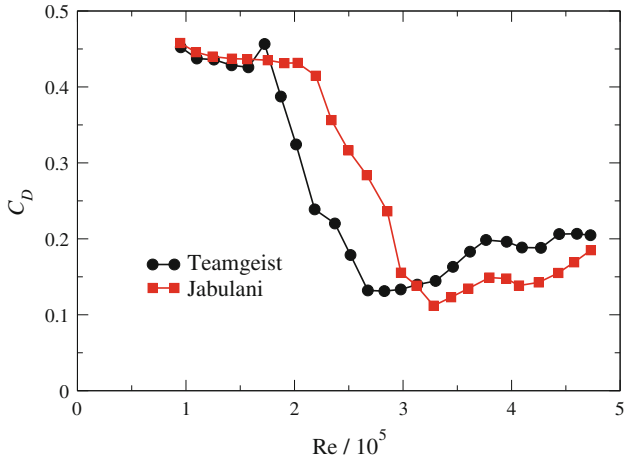

Fig. 10 Wind-tunnel drag data (Asai T, private communication) for Teamgeist and Jabulani balls. Note that Re = 10^5 corresponds to a ball speed of 6.73 m/s = 24.2 kph = 15.0 mph

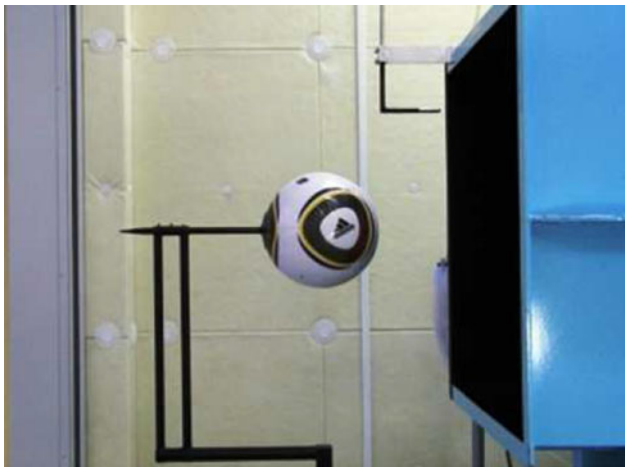

Fig. 11 Wind-tunnel set up for a Jabulani ball in a Japanese experiment (Asai T, private communication)

of an anomalous post-transition increase that has yet to be adequately explained.

An example of wind-tunnel data from Japan is shown in Fig. 10 for Teamgeist and Jabulani balls; Fig. 11 shows a Jabulani ball in the Japanese wind tunnel.

Note the implications on ball play from one World Cup to the next. As players were introduced to the Jabulani, they were given a ball that compared to the previous World Cup ball had more drag for normal playing speeds up to about 20 m/s = 72 kph = 45 mph, but less drag for larger speeds. Elite players noticed a difference in the way the Jabulani ball flew compared to balls they had used in the past.

A couple of fine wind-tunnel studies were performed in the UK. One [109] used smaller, scale models of soccer balls because of a relatively small wind tunnel. Another study [110] used regular-sized balls. Because the former study's scale model balls had sharper edges than regulation balls, the former group found smaller aerodynamic coefficients compared to the latter group, indicating that the sharper edges gave the smaller balls an overall rougher surface compared to regulation balls. Both groups noticed the reverse Magnus effect for speeds below the drag crisis and Sp < 0.3. The latter group also noticed lateral forces on nonspinning balls, forces that depend strongly on the geometry the ball presents to the wind.

Other wind-tunnel studies [111–114] have investigated differences between various ball types. Further researchers [115–118] have made great progress in the understanding of erratic knuckleball (i.e., nonspinning or very-low spin balls) trajectories. The geometry presented to the air is crucial in determining the lateral force on the ball. Researchers have used Fourier transform techniques to tease out the level of lateral force instability in various balls. There is also considerable fluctuation in the wake behind a ball with little to no spin.

To give the reader a flavor of CFD work, a couple of articles [119, 120] describe visualization of boundary-layer separation and computed aerodynamic coefficients. The CFD work is accomplished by first scanning soccer balls and then incorporating the mesh geometries into the code. Results include finding $C_D \simeq 0.15$ for a nonspinning ball beyond the drag crisis, consistent with previously discussed wind-tunnel work, and noting significant variations in lateral force with varying geometry facing the oncoming air.

Finally, though not specifically germane to this review, how players actually get the ball into its trajectory has been the subject of investigation, too. A nice review [121] of kicking looked at the entire biomechanical process of putting boot to ball, building upon older, often cited work [122] that examined ball–boot interactions form computational and experimental points of view. Recent work [123] out of Japan has specifically focused on how a boot impacts with a ball to produce a knuckleball shot.

4.16 Tennis

Besides starting with a general-audience book [124] on tennis, the beginning researcher should read the insightful review [125] of tennis ball aerodynamics that came out 5 years ago. That review shows wind-tunnel flow patterns and contains good discussions of the effect ball fuzz has on making C_D fairly large (0.6–0.7) past the drag crisis for new tennis balls. The fuzz appears to thicken the turbulent boundary layer enough to mirror that of laminar separation where the drag coefficient is relatively large.

One article not referenced directly in the review that new investigators should read is by a UK group [126]. They describe wind-tunnel measurements of C_D and C_L for

several brands of balls with various amounts of wear. Worn balls have slightly less drag, and the group showed numerically determined trajectories that illustrate the effect on play as balls wear.

Balls designed to reduce serve speed and thus slow the game down a little have been studied in a wind tunnel by an Australian group [127]. Seam orientation and geometry of ball fuzz play key roles in tennis ball aerodynamics. A UK group [128] has recently devised a method of using high-speed video and software to ascertain ball speeds and spin rates to within 10 % in a full three-dimensional treatment. What will be interesting to see in the future is a CFD analysis that accounts for ball fuzz.

4.17 Volleyball

A particularly delightful place to begin leaning about volleyball physics is with a review article [129] that came out at the close of the last millennium. US research [130] followed that review with trajectory analysis work that determined drag and lift forces. A proposed lift force that depends on speed and spin rate each to noninteger powers was proposed.

Recent wind-tunnel work out of Japan [131] compared aerodynamic properties of old and new volleyballs, the former having smooth between-seam surfaces, whereas the latter has honeycomb surfaces. The drag crisis for old balls occurs near $\mathrm{Re} = 2.7 \times 10^5$, corresponding to a speed of 19.0 m/s = 68.4 kph = 42.5 mph. For new balls, the drag crisis is near $\mathrm{Re} = 2.2 \times 10^5$, which corresponds to a speed of 15.5 m/s = 55.8 kph = 34.7 mph. The two aforementioned speeds are typical for serves and spikes, though professional hits can be 50 % or so faster. Past the drag crisis, $C_\mathrm{D} \simeq 0.17$ for new balls, large compared to $C_\mathrm{D} \simeq 0.10$ for old balls. The honeycomb design of the new balls appears to contribute to a thickening of the boundary layer, which increases drag compared to older, smoother surfaces.

4.18 Whiffle ball

Wind-tunnel work [132] in the US has been performed on Whiffle balls in various orientations. Fog was used to visualize flow and both C_D and C_L were determined as functions of ball orientation. The lift force is in the direction of the ball's holes. Because of the ball's light weight, the drag force can be nearly an order of magnitude greater than the weight as the speed reaches 37 m/s = 133 kph = 83 mph. Flow speeds inside the Whiffle ball can be about one-third what they are outside. Such a result makes a quality CFD study rather desirable.

5 Concluding remarks and a look to the future

Space limitations on this article's length make it impossible to review work done on every possible sport projectile. For some projectiles, like shot-put, racquetball, lacrosse ball, squash ball, and table tennis ball, aerodynamics are described well by approximating the objects as smooth spheres. Lacrosse balls can be manufactured with rough surfaces to reduce drag and help clubs practice with fast-moving balls. Compared to its weight, drag is not a significant force on either the hammer or the shot-put, but the steel wire attached to the hammer ball makes the aerodynamics interesting enough to include here. For a long jumper, air drag is such a small force compared to the athlete's weight, that ski jumping was the only sport reviewed here with a human projectile.

Other projectiles are similar enough to those reviewed here that young investigators are encouraged to review work here and then look for references in their chosen research area. For example, dart aerodynamics will share similarities with aerodynamics associated with an arrow and, to a slightly lesser extent, a javelin. Those researching Australian football will find similarities with American football and rugby.

There are other sport projectiles, like water polo balls, that have not been studied nearly as much as balls used in more popular sports like soccer and baseball. A water polo ball is a little smaller than a basketball, but travels at speeds comparable to basketballs. One thus expects similar aerodynamics, though the physics certainly gets more interesting with a wet ball.

With the exception of the hammer, all of the sport projectiles considered here experience drag forces that are appreciable fractions of their respective weights. Nothing comes close to the shuttlecock, which can easily feel a drag force more than 20 times its weight. A Whiffle ball may feel drag that is an order of magnitude greater than its weight. Golf balls, soccer balls, and tennis balls may all experience air drag comparable to their respective weights.

Regarding the Magnus force, essentially all projectiles considered experience some type of lift or lateral force. Baseballs, cricket balls, soccer balls, tennis balls, volleyballs, and Whiffle balls all make significant use of Magnus deflections in their respective games. A discus and a golf ball require lift for long ranges, whereas ski jumpers also make use of lift in a stabilizing way.

The exponential growth in computing power has made it possible for tyros armed only with a computer to make immediate contributions to sport aerodynamics research. As computing and data-acquisition technologies become more powerful, easier to use, and cheaper, new investigators will find that they are entering a research field that is

getting closer to the true understanding of how and why sport projectiles do what they do while in flight. More accurate CFD work is always needed; future work must better account for surface characteristics, which play a crucial role in aerodynamics. With improving high-speed camera technology, researchers are getting clearer pictures of actual flight paths. Trajectory analysis can only improve as real-world data get more accurate.

Sports with alterable playing equipment, such as soccer's World Cup having a new ball each time around, allow scientists and engineers to work with industry to develop new and better equipment. Researchers will be wise to understand material properties and how those properties influence aerodynamics. Those same researchers should also listen to what athletes have to say about how they interact with sport projectiles. Though not always equipped with scientific jargon, athletes can teach scientists a great deal about how balls and other sport objects move, and athletes are often a fantastic source of new research ideas.

Acknowledgments I thank Matt Carré for providing me with some pertinent articles. I also thank Jay Gerlach for providing me with journal access at his university. Thanks to Matthew Jones and Michael Solontoi for reading an early draft and offering helpful comments. I am also grateful to reviewers for valuable suggestions.

References

1. Daish CB (1972) The physics of ball games. The English Universities Press Ltd, London
2. Mehta RD (1985) Aerodynamics of sports balls. Ann Rev Fluid Mech 17:151–189
3. Frohlich C (2011) Resource Letter PS-2: Physics of Sports. Am J Phys 79:565–574
4. White C (2011) Projectile dynamics in sport. Routledge, Abingdon
5. Wolfson R (2012) Essential University Physics, 2nd edn. Addison-Wesley, San Francisco, p 40
6. http://www.hittrackeronline.com
7. Thornton ST, Marion JB (2004) Classical dynamics of particles and systems, 5th edn. Thomson Brooks/Cole, Belmont, p 59
8. Goff JE (2004) Heuristic model of air drag on a sphere. Phys Educ 39:496–499
9. Adair RK (2002) The physics of baseball, 3rd edn. Perennial/Harper Collins, New York
10. White FM (2011) Fluid mechanics, 7th edn. McGraw-Hill Higher Education, New York
11. Wesson J (2002) The science of soccer. Institute of Physics Publishing, London, p 168
12. Goff JE, Carré MJ (2009) Trajectory analysis of a soccer ball. Am J Phys 77:1020–1027
13. Watts RG, Bahill AT (2000) Keep your eye on the ball: curve balls, knuckleballs, and fallacies of baseball (revised and updated). WH Freeman and Co, New York
14. Nathan AM (2008) The effect of spin on the flight of a baseball. Am J Phys 76:119–124
15. de Mestre N (1990) The mathematics of projectiles in sport. Cambridge University Press, Cambridge
16. Anderson Jr JD (2005) Ludwig Prandtl's Boundary Layer. Phys Today 58:42–48
17. Achenbach E (1972) Experiments on the flow past spheres at very high Reynolds numbers. J Fluid Mech 54:565–575
18. Goff JE (2010) Power and spin in the beautiful game. Phys Today 63:62–63
19. Bearman PW and Harvey JK (1976) Golf Ball Aerodynamics. Aeronautical Quarterly 27:112–122
20. Achenbach E (1974) The effects of surface roughness and tunnel blockage on the flow past spheres. J Fluid Mech 65:113–125
21. Haake SJ, Goodwill SR, Carré MJ (2007) A new measure of roughness for defining the aerodynamic performance of sports balls. Proc IMechE, Part C: J Mech Eng Sci 221:789–806
22. Koonin SE, Meredith DC (1990) Computational physics. Addison-Wesley, Boston Chapter 6
23. Huebner KH (2001) The finite element method for engineers, 4th edn. Wiley-Interscience, New York
24. Beer G, Smith I, Duenser C (2008) The boundary element method with programming: for engineers and scientists. Springer, New York
25. Hanna RK (2012) CFD in Sport – a Retrospective; 1992–2012. Proc Eng 34:622–726
26. Chung TJ (2010) Computational fluid dynamics, 2nd edn. Cambridge University Press, Cambridge
27. http://www.huffingtonpost.com/2012/08/03/archery-olympics-hunger-games-london_n_1738182.html. Accessed Jan 2013
28. Klopsteg PE (1943) Physics of Bows and Arrows. Am J Phys 11:175–192
29. Denny M (2011) Their arrows will darken the sun: the evolution and science of ballistics. The Johns Hopkins University Press, Baltimore
30. French K and Kirk T (2005) Measuring the flight of an arrow using the Acoustic Doppler Shift. Mech Sys and Sig Proc 21:1188–1191
31. Park JL (2010) The behaviour of an arrow shot from a compound archery bow. Proc Inst Mech Eng Part P J Sports Eng and Tech 225:8–21
32. Park JL, Hodge MR, Al-Mulla S, Sherry M, Sheridan J (2011) Air flow around the point of an arrow. Proc Inst Mech Eng Part P J Sports Eng Tech (published online 15 Dec 2011)
33. Park JL (2011) The aerodynamic drag and axial rotation of an arrow. Proc Inst Mech Eng Part P J Sports Eng and Tech 225:199–211
34. Miyazaki T, Mukaiyama K, Komori Y, Okawa K, Taguchi S, Sugiura H (2012) Aerodynamic properties of an archery arrow. Sports Eng (published online 10 Oct 2012)
35. Barton J, Včelák J, Torres-Sanchez J, O'Flynn B, O'Mathuna C, and Donahoe RV (2012) Arrow-mounted Ballistic System for Measuring Performance of Arrows Equipped with Hunting Broadheads. Proc Eng 34:455–460
36. Rieckmann M, Park JL, Codrington J, Cazzolato B (2012) Modeling the 3D vibration of composite archery arrows under free-free boundary conditions. Proc Inst Mech Eng P J Sports Eng Techn 226:114–122
37. Chen LM, P YH, Chen YJ (2009) A study of shuttlecock's trajectory in badminton. J Sports Sci and Med 8:657–662
38. Alam F, Chowdhury H, Theppadungporn C, and Subic A (2010) Measurements of Aerodynamic Properties of Badminton Shuttlecocks. Proc Eng 2:2487–2492
39. Chan CM, Rossmann JS (2012) Badminton shuttlecock aerodynamics: synthesizing experiment and theory. Sports Eng 15:61–71
40. Nakagawa K, Hasegawa H, Murakami M, Obayashi S (2012) Aerodynamic Properties and Flow Behavior for a Badminton Shuttlecock with Spin at High Reynolds Numbers. Proc Eng 34:104–109

41. Texier BD, Cohen C, Quéré D, and Claneta C (2012) Shuttlecock dynamics. Proc Eng 34:176–181
42. Briggs LJ (1959) Effect of Spin and Speed on the Lateral Deflection (Curve) of a Baseball; and the Magnus Effect for Smooth Spheres. Am J Phys 27:589–596
43. Alawys LW, Hubbard M (2001) Experimental determination of baseball spin and lift. J Sports Sci 19:349–358
44. Sawicki GS, Hubbard M, Stronge WJ (2003) How to hit home runs: Optimum baseball bat swing parameters for maximum range trajectories. Am J Phys 71:1152–1162
45. McBeath MK, Nathan AM, Bahill AT, Baldwin DG (2008) Paradoxical pop-ups: Why are they difficult to catch? Am J Phys 76:723–729
46. www.sportvision.com/baseball/pitchfx.Accessed Jan 2013
47. Nathan AM (2012) Analysis of knuckleball trajectories. Proc Eng 34:116–121
48. Meyer ER, Bohn JL (2008) Influence of a humidor on the aerodynamics of baseballs. Am J Phys 76:1015–1021
49. Nathan AM, Cantakos J, Kesmna R, Mathew B, Lukash W (2012) Spin of a batted baseball. Proc Eng 34:182–187
50. McGinnis RS, Perkins NC, King K (2012) Pitcher training aided by instrumented baseball. Proc Eng 34:580–585
51. Fontanella JJ (2006) The physics of basketball, The Johns Hopkins University Press, Baltimore
52. Huston RL, Grau CA (2003) Basketball shooting strategies – the free throw, direct shot and layup. Sports Eng 6:49–64
53. Okubo H, Hubbard M (2012) Defense for basketball field shots. Proc Eng 34:730–735
54. Mehta RD (2005) An overview of cricket ball swing. Sports Eng 8:181–192
55. James DM, Carré MJ, and Haake SJ (2004) The playing performance of country cricket pitches. Sports Eng 7:1–14
56. James D, MacDonald DC, and Hart J (2012) The effect of atmospheric conditions on the swing of a cricket ball. Proc Eng 34:188–193
57. Fuss FK, Smith RM, Subic A (2012) Determination of spin rate and axes with an instrumented cricket ball. Proc Eng 34:128–133
58. Penrose JMT, Hose DR, Trowbridge EA (1996) Cricket ball swing: a preliminary analysis using computational fluid dynamics. In: Haake (ed) The engineering of sport. AA Balkema, Rotterdam, pp 11–19
59. Hubbard M, Cheng KB (2007) Optimal discus trajectories. J Biomech 40:3650–3659
60. Frohlich C (1981) Aerodynamic and mechanical forces in discus flight. Am J Phys 49:1125–1132
61. Goff JE (2010) Gold medal physics: the science of sports. The Johns Hopkins University Press, Baltimore, Chapter 8
62. Seo K, Shimoyama K, Ohta K, Ohgi Y, Kimura Y (2012) Aerodynamic behavior of a discus. Proc Eng 34:92–97
63. Crowther WJ, Potts JR (2007) Simulation of a spin-stabilised sports disc. Sports Eng 10:3–21
64. Lissaman P, Hubbard M (2010) Maximum range of flying discs. Proc Eng 2:2529–2535
65. Gay T (2005) The physics of football. HarperCollins, New York
66. Goff JE (2010) Gold medal physics: the science of sports. The Johns Hopkins University Press, Baltimore, Chapter 3
67. Rae WJ (2003) Flight dynamics of an American football in a forward pass. Sports Eng 6:149–163
68. Rae WJ, Steit RJ (2002) Wind-tunnel measurements of the aerodynamic loads on an American football. Sport Eng 5:165–172
69. Alam F, Smith S, Chowdhury H, and Moria H (2012) Aerodynamic drag measurements of American footballs. Proc Eng 34:98–103
70. Watts RG, Moore G (2003) The drag on an American football. Am J Phys 71:791–793
71. Jorgensen TP (1999) The physics of golf, 2nd edn. Springer, New York
72. Davies JM (1949) The Aerodynamics of Golf Balls. J Appl Phys 20:821–828
73. Choi J, Jeon WP, Choi H (2006) Mechanism of drag reduction by dimples on a sphere. Phys Fluids 18:041702
74. Penner AR (2001) The physics of golf: The optimum loft of a driver. Am J Phys 69:563–568
75. Penner AR (2001) The physics of golf: The convex face of a driver. Am J Phys 69:1073–1081
76. Parviz M, Kim J (1997) Tackling Turbulence with Supercomputers. Sci Am 276:62–68
77. Tanaka K, Teranishi Y, Ujihashi S (2010) Experimental and finite element analyses of a golf ball colliding with a simplified club during a two-dimensional swing. Proc Eng 2:3249–3254
78. Dapena J, Gutiérrez-Dávila G, Soto VM, Rojas FJ (2003) Prediction of distance in hammer throwing. J Sports Sci 21:21–28
79. Haché A (2002) The physics of hockey. The Johns Hopkins University Press, Baltimore
80. Böhm H, Schwiewagner C, and Senner V (2007) Simulation of puck flight to determine spectator safety for various ice hockey board heights. Sports Eng 10:75–86
81. Hubbard M, Rust HJ (1984) Simulation of Javelin Flight Using Experimental Aerodynamic Data. J Biomech 17:769–776
82. Hubbard M (1984) Optimal Javelin Trajectories. J Biomech 17:777–787
83. Hubbard M, Alaways LW (1987) Optimum Release Conditions for the New Rules Javelin. Int J Sport Biomech 3:207–221
84. Hubbard M, Bergman CD (1989) Effect of Vibrations on Javelin Lift and Drag. Int J Sport Biomech 5:40–59
85. Hubbard M, Laport S (1997) Damping of Javelin Vibrations in Flight. J Appl Biomech 13:269–286
86. Maryniak J, Ladyźyńska-Kozdraś E, Golińska E (2009) Mathematical Modeling and Numerical Simulations of Javelin Throw. Hum Dev 10:16–20
87. Maszczyk A, Zając A, Ryguła I (2011) A neural network model approach to athlete selection. Sports Eng 13:83–93
88. Lipscombe TD (2009) The physics of rugby. Nottingham University Press, Nottingham
89. Seo K, Kobayashi O, Murakami M (2006) Flight dynamics of the screw kick in rugby. Sports Eng 9:49–58
90. Alam F, Subic A, Watkins S, Smits AJ (2010) Aerodynamics of an Australian rules foot ball and rugby ball. In: Peters M (ed) Computational fluid dynamics for sport simulation. Springer, Berlin
91. Djamovski V, Rosette P, Chowdhury H, Alam F, Steiner T (2012) A comparative study of rugby ball aerodynamics. Proc Eng 34:74–79
92. Taha Z, Sugiyono (2009) Effect of diameter on the aerodynamics of sepaktakraw balls, a computational study. Int J Sports Sci Eng 3:17–21
93. Seo K, Watanabe I, Murakami M (2004) Aerodynamic force data for a V-style ski jumping flight. Sports Eng 7:31–39
94. Seo K, Murakami M, Yoshida K (2004) Optimal flight technique for V-style ski jumping. Sports Eng 7:97–104
95. Nørstrud H, Øye IJ (2010) On CFD simulation of ski jumping. In: Peters M (ed) Computational fluid dynamics for sport simulation. Springer, Berlin
96. McNeil JA, McNeil JB (2009) Dynamical analysis of winter terrain park jumps. Sports Eng 11:159–164
97. McNeil JA, Hubbard M, Swedberg AD (2012) Designing tomorrow's snow park jump. Sports Eng 15:1–20
98. Chardonnens J, Favre J, Callennec BL, Cuendet F, Gremion G, Aminian K (2012) Automatic measurement of key ski jumping phases and temporal events with a wearable system. J Sports Sci 30:53–61

99. Goff JE (2010) Gold medal physics: the science of sports. The Johns Hopkins University Press, Baltimore, Chapter 7
100. Carré MJ, Asai T, Akatsuka T, Haake SJ (2002) The curve kick of a football II: flight through the air. Sports Eng 5:193–200
101. Goff JE, Carré MJ (2010) Soccer ball lift coefficients via trajectory analysis. Euro J Phys 31:775–784
102. Barber S, Carré MJ (2010) The effect of surface geometry on soccer ball trajectories. Sports Eng 13:47–55
103. Myers TG, Mitchell SL (2012) A mathematical analysis of the motion of an in-flight soccer ball. Sports Eng (published online 16 October 2012)
104. Bray K, Kerwin DG (2003) Modelling the flight of a soccer ball in a direct free kick. J Sports Sci 21:75–85
105. Cook BG, Goff JE (2006) Parameter space for successful soccer kicks. Euro J Phys 27:865–874
106. Asai T, Seo K, Kobayashi O, Sakashita R (2007) Fundamental aerodynamics of the soccer ball. Sports Eng 10:101–110
107. Goff JE, Smith WH, Carré MJ (2011) Football boundary-layer separation via dust experiments. Sports Eng 14:139–146
108. Goff JE, Carré MJ (2012) Investigations into soccer aerodynamics via trajectory analysis and dust experiments. Proc Eng 34:158–163
109. Carré MJ, Goodwill SR, Haake SJ (2005) Understanding the effect of seams on the aerodynamics of an association football. Proc IMechE, Part C: J Mech Eng Sci 219:657–666
110. Passmore MA, Tuplin S, Spencer A, Jones R (2008) Experimental studies of the aerodynamics of spinning and stationary footballs. Proc IMechE, Part C: J Mech Eng Sci 222:195–205
111. Alam F, Chowdhury H, Moria H, Fuss FK (2010) A comparative study of football aerodynamics. Proc Eng 2:2443–2448
112. Alam F, Chowdhury H, Moria H, Fuss FK, Khan I, Aldawi F, Subic A (2011) Aerodynamics of contemporary FIFA soccer balls. Proc Eng 13:188–193
113. Asai T, Ito S, Seo K, Koike S (2012) Characteristics of modern soccer balls. Proc Eng 34:122–127
114. Alam F, Chowdhury H, Stemmer M, Wang Z, Yang J (2012) Effects of surface structure on soccer ball aerodynamics. Proc Eng 34:146–151
115. Hong S, Chung C, Nakayama M, Asai T (2010) Unsteady Aerodynamic Force on a Knuckleball in Soccer. Proc Eng 2:2455–2460
116. Asai T, Kamemoto K (2011) Flow structure of knuckling effects in footballs. J Fluids Struc 27:727–733
117. Murakami M, Seo K, Kondoh M, Iwai Y (2012) Wind tunnel measurement and flow visualisation of soccer ball knuckle effect. Sports Eng 15:29–40
118. Ito S, Kamata M, Asai T, Seo K (2012) Factors of unpredictable shots concerning new soccer balls. Proc Eng 34:152–157
119. Barber S, Chin SB, Carré MJ (2009) Sports ball aerodynamics: a numerical study of the erratic motion of soccer balls. Comput Fluids 38:1091–1100
120. Barber S, Carré MJ (2010) Soccer ball aerodynamics. In: Peters M (ed) Computational fluid dynamics for sport simulation. Springer, Berlin
121. Lees A, Asai T, Andersen TB, Nunome H, Sterzing T (2010) The biomechanics of kicking in soccer: A review. J of Sports Sci 28:805–817
122. Asai T, Carré MJ, Akatsuka T, Haake SJ (2002) The curve kick of a football I: impact with the foot. Sports Eng 5:183–192
123. Hong S, Kazama Y, Nakayama M, Asai T (2012) Ball impact dynamics of knuckling shot in soccer. Proc Eng 34:200–205
124. Cross R, Lindsey C (2004) Technical tennis: racquests, strings, balls, courts, spin, and bounce. USRSA, Duluth
125. Mehta RD, Alam F, Subic A (2008) Aerodynamics of tennis balls – a review. Sports Tech 1:1–10
126. Goodwill SR, Chin SB, Haake SJ (2004) Aerodynamics of a spinning and non-spinning tennis balls. J Wind Eng 92:935–958
127. Djamovski V, Pateras J, Chowdhury H, Alam F, Steiner T (2012) Effects of seam and surface texture on tennis balls aerodynamics. Proc Eng 34:140–145
128. Kelley J, Choppin SB, Goodwill SR, Haake SJ (2010) Validation of a live, automatic ball velocity and spin rate finder in tennis. Proc Eng 2:2967–2972
129. Cairns TW, Van Lierop K (2000) Volleyballs and Aerodynamics: A Review. Int J Volleyball Res 3:8–14
130. Cairns TW (2004) Modeling lift and drag forces on a volleyball. In: Hubbard M, Mehta RD, Pallis JM (eds) The engineering of sport 5, vol 1, pp 97–103
131. Asai T, Ito S, Seo K, Hitotsubashi A (2010) Aerodynamics of a New Volleyball. Proc Eng 2:2493–2498
132. Rossmann Jenn, Rau A (2007) An experimental study of Whiffle ball aerodynamics. Am J Phys 75:1099–1105